Copy
RM L55L14

NACA RM L55L14

3 1176 00072 9849

NACA FOR REFERENCE

NOT TO BE TAKEN FROM THIS ROOM

RESEARCH MEMORANDUM

PRELIMINARY MEASUREMENTS OF THE AERODYNAMIC YAWING DERIVATIVES OF A TRIANGULAR, A SWEPT, AND AN UNSWEPT WING PERFORMING PURE YAWING OSCILLATIONS, WITH A DESCRIPTION OF THE INSTRUMENTATION EMPLOYED

By M. J. Queijo, Herman S. Fletcher,
C. G. Marple, and F. M. Hughes

Langley Aeronautical Laboratory
Langley Field, Va.

CLASSIFICATION CHANGED
UNCLASSIFIED

NACA Res Abs
Notice of RN-116 Date effective June 20, 1957
CLASSIFIED DOCUMENT
ad 7-10-57

This material contains information affecting the National Defense of the United States within the meaning of the espionage laws, Title 18, U.S.C., Secs. 793 and 794, the transmission or revelation of which in any manner to an unauthorized person is prohibited by law.

NATIONAL ADVISORY COMMITTEE
FOR AERONAUTICS

WASHINGTON

April 2, 1956

[redacted]

NATIONAL ADVISORY COMMITTEE FOR AERONAUTICS

RESEARCH MEMORANDUM

PRELIMINARY MEASUREMENTS OF THE AERODYNAMIC YAWING DERIVATIVES OF A TRIANGULAR, A SWEPT, AND AN UNSWEPT WING PERFORMING PURE YAWING OSCILLATIONS, WITH A DESCRIPTION OF THE INSTRUMENTATION EMPLOYED

By M. J. Queijo, Herman S. Fletcher,
C. G. Marple, and F. M. Hughes

SUMMARY

A preliminary investigation has been made to determine the effect of motion periodicity on the aerodynamic derivatives due to yawing velocity and yawing acceleration for a 60° delta wing, a 45° sweptback wing, and an unswept wing. Results were obtained from steady-state yawing-flow tests and from tests of the models performing pure sinusoidal yawing oscillations. The oscillation tests were made at one value of the reduced-frequence parameter, $\omega b/2V = 0.23$. Tests of models on other oscillating systems have shown a large dependence of some derivatives on the reduced frequency, particularly at high angles of attack; hence this fact should be kept in mind in considering the following statements. The results showed that at low angles of attack there was good agreement between steady-state and oscillatory values of the aerodynamic derivatives due to yawing velocity for all three wings. At high angles of attack large differences occurred between steady-state and oscillatory values of the derivatives due to yawing velocity for all three wings. The derivatives due to yawing acceleration varied approximately linearly with angle of attack in the low angle-of-attack range. At angles of attack near and above maximum lift, these derivatives showed no linear dependence on angle of attack and attained large numerical values.

A description of the design and function of the instrumentation used in the investigation is included in the appendix.

[redacted]

INTRODUCTION

The advent of high-speed airplanes of high relative density has focused attention on certain problems associated with the dynamic stability of aircraft which, because of previous unimportance, have heretofore been neglected. Among the problems are the effect of periodicity of the airplane motion on the stability derivatives, and the possibility that acceleration derivatives (which generally have been neglected when making dynamic stability calculations) may be important for certain airplane configurations.

Some information on both problems already has been obtained experimentally. References 1 through 3, for example, show comparisons between damping-in-yaw derivatives obtained from steady-state tests performed by use of the Langley stability tunnel curved-flow technique and from tests in which the models were oscillated about their vertical axes. The former technique permits measurements of the derivatives due to yawing velocity, for example the yawing moment due to yawing velocity C_{n_r}. The latter technique permits measurement of a combination of damping derivatives $\left(C_{n_{r,\omega}} - C_{n_{\dot{\beta},\omega}}\right)$. A comparison of results from the two techniques for the same model under identical conditions indicates the approximate magnitude of the sideslip acceleration derivative $C_{n_{\dot{\beta},\omega}}$. Such comparative tests have indicated that for certain configurations the derivatives associated with acceleration in sideslip can be quite large at high angles of attack. Direct measurement of the sideslip acceleration derivatives (reference 4) have, of course, substantiated the results of the comparative tests.

There is little experimental data available on the effect of motion periodicity on aerodynamic derivatives associated with linear or angular velocity. Recent tests on a series of wings performing lateral plunging oscillations across the jet of a tunnel (ref. 4) have permitted evaluation of the derivatives associated with sideslip velocity during a sinusoidal sideslip oscillation. These results indicated that for a 60° delta and a 45° sweptback wing at high angles of attack the sideslip derivatives extracted from lateral oscillation tests were much different from the derivatives obtained by the usual steady-state wind-tunnel procedures.

As a continuation of the program to determine effects of motion periodicity on the various stability derivatives, the present investigation was made to determine the derivatives associated with yawing velocity and yawing acceleration by use of an apparatus which simulated a pure yawing oscillation. Data also were obtained from steady-state yawing tests by use of the Langley stability tunnel curved-flow technique for comparison with the oscillation data.

[redacted]

SYMBOLS

The data presented herein are referred to the stability system of axes with the origin located at the quarter chord of the mean aerodynamic chord. The positive directions of forces, moments, and displacements are shown in figure 1. The coefficients and symbols are defined as follows:

b	wing span
c	wing chord
$\bar{c}$	wing mean aerodynamic chord, $\frac{2}{S}\int_0^{b/2} c^2 dy$
D	drag
f	frequency
I_Z	model moment of inertia about the Z axis
l	distance between flywheel centers
I_{XZ}	product of inertia
L	lift
L'	rolling moment
M	pitching moment
N	yawing moment
q	dynamic pressure, $\frac{1}{2}\rho V^2$
r	angular velocity in yaw, $(r = \dot{\psi})$, radian/sec
R	throw of flywheels of oscillating mechanism (see fig. 2)
S	wing area
t	time, sec
V	free-stream velocity
y	distance along y-axis, measured from wing plane of symmetry

[redacted]

y' distance between model mounting point and center of drive flywheel

Y lateral force

C_D drag coefficient, D/qS

C_L lift coefficient, L/qS

C_l rolling-moment coefficient, L'/qSb

C_m pitching-moment coefficient, $M/qS\bar{c}$

C_n yawing-moment coefficient, N/qSb

C_Y lateral-force coefficient, Y/qS

α angle of attack, deg

ψ yaw angle, rad

ρ mass density of air

$\dot{r} = \frac{\partial r}{\partial t}$

$\dot{\psi} = \frac{\partial \psi}{\partial t}$

$\ddot{\psi} = \frac{\partial^2 \psi}{\partial t^2}$

$l_{\dot{\psi}} = \frac{\partial l}{\partial \dot{\psi}}$

$l_{\ddot{\psi}} = \frac{\partial l}{\partial \ddot{\psi}}$

$N_{\dot{\psi}} = \frac{\partial N}{\partial \dot{\psi}}$

[redacted]

$$N_{\ddot{\psi}} = \frac{\partial N}{\partial \ddot{\psi}}$$

$$C_{l_r} = \frac{\partial C_l}{\partial \frac{rb}{2V}}$$

$$C_{n_r} = \frac{\partial C_n}{\partial \frac{rb}{2V}}$$

$$C_{n_{\dot{r}}} = \frac{\partial C_n}{\partial \frac{\dot{r}b^2}{4V^2}}$$

$$C_{l_{\dot{r}}} = \frac{\partial C_l}{\partial \frac{\dot{r}b^2}{4V^2}}$$

$$\dot{y}' = \frac{\partial y'}{\partial t}$$

$$\dot{y} = \frac{\partial y}{\partial t}$$

The subscript ω when used with a derivative (for example, $C_{l_{r,\omega}}$) indicates that the derivative was obtained from an oscillation test.

APPARATUS

Oscillation Tests

The tests of the present investigation were conducted in the 6- by 6-foot test section of the Langley stability tunnel. The oscillation equipment constructed for the investigation was designed to simulate

[redacted]

a pure yawing oscillation. A pure yawing oscillation is an oscillatory motion in the x-y plane such that the airplane is always heading into the relative wind - or, more specificially, it is an oscillatory motion in the x-y plane such that there is no resultant lateral velocity component at the airplane center of gravity. The following sketch illustrates the path and attitude of an airplane performing a sinusoidal yawing oscillation:

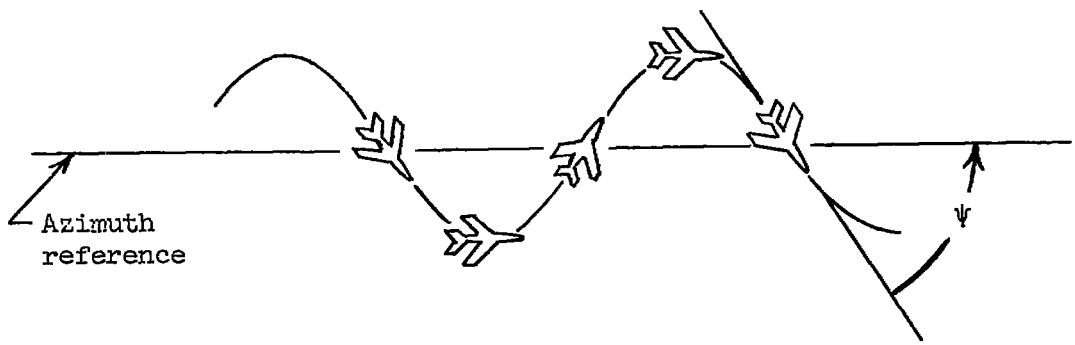

For a model mounted in a wind tunnel such a motion corresponds to the proper superposition of a yawing oscillation about the vertical axis, a lateral sideslip oscillation, and the free-stream tunnel velocity. The condition of no lateral resultant velocity at the assumed model center of gravity (or mounting point) is met when

$$V \sin \psi = \dot{y} \tag{1}$$

This condition was approximated in the present investigation by use of the apparatus shown schematically in figure 2. Photographs of the actual apparatus are given as figure 3. The model was attached to a strain-gage balance which was in turn fastened to a support system consisting primarily of one large streamline tube. The streamline tube was supported at the ends by flywheels, which were driven by means of various shafts, gears, and a variable-frequency motor-generator set. The flywheels rotate in opposite directions, hence the yaw angle of the model at any instant is given by

$$\tan \psi = \frac{-2R \sin 2\pi ft}{l}$$

or

$$\sin \psi = \frac{-2R \sin 2\pi ft}{\sqrt{l^2 + 4R^2 \sin^2 2\pi ft}} \tag{2}$$

The distance between the model mounting point and the center of the drive flywheel is

$$y' = \frac{l}{2} \cos \psi - R \cos 2\pi ft$$

or

$$y' = \frac{l^2}{2\sqrt{l^2 + 4R^2 \sin^2 2\pi ft}} - R \cos 2\pi ft \tag{3}$$

hence the velocity of the model toward the drive flywheel is

$$\dot{y}' = -\left[- \frac{2Rl^2 \cos 2\pi ft}{\left(l^2 + 4R^2 \sin^2 2\pi ft\right)^{3/2}} + 1 \right] (2\pi fR \sin 2\pi ft)$$

The model sideslip velocity is

$$\dot{y} = \dot{y}' \cos \psi$$

or

$$\dot{y} = -\left[- \frac{2Rl^2 \cos 2\pi ft}{\left(l^2 + 4R^2 \sin^2 2\pi ft\right)^{3/2}} + 1 \right] (2\pi fR \sin 2\pi ft) \frac{l}{\sqrt{l^2 + 4R^2 \sin^2 2\pi ft}} \tag{4}$$

Substitution of equations (2) and (4) into equation (1) yields

[redacted]

$$V = \left[- \frac{2Rl^2 \cos 2\pi ft}{\left(l^2 + 4R^2 \sin^2 2\pi ft\right)^{3/2}} + 1 \right] \pi f l^2$$

which, for the mechanism sketched in figure 2, is the relationship between V and f for a pure yawing oscillation. This variation is rather complex since V is to some extent dependent on angular position of the flywheels as indicated by the first term within the bracket. The effect of this term can be minimized by making l large relative to R which is, of course, a restriction on the magnitude of the yaw angle. In the present investigation R was 12 inches and l was 156 inches, hence the magnitude of the term within the bracket varied from 0.85 to 1.15. An average value of 1.00 was used throughout the investigation so that the relationship between V and f was given by

$$V = \pi f l \tag{5}$$

The yawing and rolling moments acting on the models during the tests were measured by means of a strain-gage balance. The signals from the strain gage were passed into instrumentation which permitted direct measurement of quantities proportional to the moments due to yawing velocity and acceleration. The instrumentation used in these tests was designed and assembled by Messrs. C. G. Marple, and F. M. Hughes of the Langley Instrument Research Division. A description of the design and function of the instrumentation, prepared by them, is given in the appendix.

Steady-State Tests

The steady-state yawing tests were conducted in the Langley stability tunnel by use of the curved-flow technique wherein the airstream is made to curve about a fixed model (see ref. 5). The model was attached to a single-strut support system which was in turn fastened to a 6-component electro-mechanical balance.

MODELS

The models used in this investigation were those previously used in the investigation of reference 4 and consisted of a 60° triangular, a 45° sweptback, and an unswept wing. The swept and unswept wings had aspect ratios of 4.0, and taper ratios of 0.6. Each wing was constructed

from 3/4-inch plywood and had a flat-plate airfoil section with a circular leading edge and a beveled trailing edge. The trailing edges of all wings were beveled to provide a trailing-edge angle of 10° across the span. Sketches of the three wings and their geometric characteristics are presented in figure 4.

Before testing the models, each wing was lightened and statically balanced about the mounting point to reduce inertia effects insofar as possible. A canopy which was used on the wings (fig. 3(b)) was made of balsa and served to streamline the protrusion of the strain-gage balance above the upper surface of the models at angles of attack. The lead weight shown attached to the center of the wing leading edge was required for static balance of the unswept wing about the yaw (Z) axis. All openings in the canopies were sealed to prevent leakage of air through the model.

TESTS

All tests of this investigation were made in the 6- by 6-foot test section of the Langley stability tunnel. The oscillation tests were made at a dynamic pressure of 16 pounds per square foot and at a reduced frequency $\omega b/2V$ of 0.23, a value which was fixed by the mechanics of the apparatus used to simulate a pure yawing motion of the model. The steady-state yawing-flow tests were made at a dynamic pressure of 24.9 pounds per square foot and at airstream curvatures corresponding to values of $rb/2V$ of 0, -0.0311, -0.0660, and -0.0869.

The Reynolds numbers for the tests, based on the wing mean aerodynamic chord, and the angle-of-attack range for each wing were as follows:

Wing	Dynamic pressure	Reynolds number based on c	Angle-of-attack range
60° Δ	16	1,262,000	0 to 32°
45° sweptback	16	558,000	0 to 32°
Unswept	16	558,000	0 to 16°
60° Δ	24.9	1,580,000	0 to 32°
45° sweptback	24.9	696,000	0 to 32°
Unswept	24.9	696,000	0 to 16°

[redacted]

CORRECTIONS

Jet boundary corrections to angle of attack and drag coefficient, determined by the method of reference 6 and based on the data obtained from the steady-yawing-flow tests at $rb/2V = 0$, have been applied to both the steady-state and oscillatory results. No corrections were applied to the oscillatory derivatives because they were felt to be small (ref. 7). The resonance effects discussed in reference 8 become important, for the frequency considered herein, only at Mach numbers near unity, and thus require no consideration for the present investigation. The data have not been corrected for blockage, turbulence, or support interference although the latter may have a sizeable magnitude at the higher angles of attack.

REDUCTION OF OSCILLATION TEST DATA

The equations of motion for a model performing a forced sinusoidal yawing oscillation are

$$N_{\dot{\psi}}\dot{\psi} + N_{\ddot{\psi}}\ddot{\psi} + B \sin 2\pi ft + C \cos 2\pi ft = I_z\ddot{\psi} \tag{6}$$

about the z axis, and

$$l_{\dot{\psi}}\dot{\psi} + l_{\ddot{\psi}}\ddot{\psi} + D \sin 2\pi ft + E \cos 2\pi ft = -I_{xz}\ddot{\psi} \tag{7}$$

about the x axis, where B and D are the maximum in-phase yawing and rolling moments respectively, and C and E the corresponding out-of-phase moments supplied by the strain gage. The yaw angle of the model in the present tests was given by equation (2), which for small yaw angles can be written as

$$\psi = -\frac{2R}{l} \sin 2\pi ft$$

from which

$$\dot{\psi} = -\frac{4\pi fR}{l} \cos 2\pi ft \tag{8}$$

[redacted]

and

$$\ddot{\psi} = \frac{8\pi^2 f^2 R}{l} \sin 2\pi f t \tag{9}$$

Substituting equations (8) and (9) into equations (6) and (7) and separating the moments which are in-phase and out-of-phase with respect to the yaw angle ψ yields

$$\left.\begin{aligned} N_{\dot{\psi}} &= \frac{Cl}{4\pi f R} && \text{(Out-of-phase)} \\ N_{\ddot{\psi}} &= I_z - \frac{Bl}{8\pi^2 f^2 R} && \text{(In-phase)} \\ l_{\dot{\psi}} &= \frac{El}{4\pi f R} && \text{(Out-of-phase)} \\ l_{\ddot{\psi}} &= -I_{xz} - \frac{Dl}{8\pi^2 f^2 R} && \text{(In-phase)} \end{aligned}\right\} \tag{10}$$

In coefficient form equations (10) become

$$\left.\begin{aligned} C_{n_r} &= \frac{C}{\pi^2 f^2 R \rho S b^2} \\ C_{n_{\dot{r}}} &= \frac{8I_z}{\rho S b^3} - \frac{Bl}{\pi^2 f^2 R \rho S b^3} \\ C_{l_r} &= \frac{E}{\pi^2 f^2 R \rho S b^2} \\ C_{l_{\dot{r}}} &= -\frac{8I_{xz}}{\rho S b^3} - \frac{Dl}{\pi^2 f^2 R \rho S b^3} \end{aligned}\right\} \tag{11}$$

[redacted]

In the present tests the moments B, C, D, and E were measured for the wind-on and wind-off conditions by the electronic equipment described in the appendix; hence the coefficients were readily obtained from the following equations:

$$\left.\begin{aligned} C_{n_r} &= \frac{C_{\text{wind on}} - C_{\text{wind off}}}{\pi^2 f^2 R\rho S b^2} \\ C_{l_r} &= \frac{E_{\text{wind on}} - E_{\text{wind off}}}{\pi^2 f^2 R\rho S b^2} \\ C_{n_{\dot{r}}} &= -\frac{B_{\text{wind on}} - B_{\text{wind off}}}{\pi^2 f^2 R\rho S b^3} \\ C_{l_{\dot{r}}} &= -\frac{D_{\text{wind on}} - D_{\text{wind off}}}{\pi^2 f^2 R\rho S b^3} \end{aligned}\right\} \qquad (12)$$

As is shown in the appendix, the instrumentation used in this investigation yielded readings on a voltmeter $\bar{e}_n$ or $\bar{e}_l$ directly proportional to the yawing and rolling moments, hence the aerodynamic moments B, C, D, and E could be obtained readily and used with equations (12) to obtain the desired aerodynamic derivatives.

RESULTS AND DISCUSSION

The results of this investigation are presented in figures 5, 6, and 7 as curves of the various parameters plotted against angle of attack. Recent investigations of derivatives measured on oscillating models have shown a large dependence of some derivatives on reduced frequency, particularly at high angles of attack (refs. 4 and 9), hence the results of the present oscillatory tests, made at one value of reduced frequency, would probably be modified by frequency changes.

Static Longitudinal Characteristics

The static longitudinal characteristics of the three models are presented in figure 5 as curves of C_L, C_D, and C_m plotted against

angle of attack. These data have been presented and discussed in reference 4 and therefore are not discussed herein, but are included primarily to relate the lift to angle of attack.

Derivatives Due to Yawing Velocity

The derivatives associated with yawing velocity, C_{n_r}, C_{l_r}, and C_{y_r} from the oscillatory and steady-state tests are given in figure 6 as functions of the angle of attack for the three wings tested. In general, the steady-state and oscillatory values of the parameters C_{n_r} and C_{l_r} are in good agreement at low angles of attack for all three wings. At high angles of attack, however, the steady-state and oscillatory values of these parameters are very different in magnitude, and often also in sign. For example at an angle of attack of 20° for the 45° sweptback wing the steady-state value of C_{l_r} is -0.02, whereas the oscillatory value is 0.30. The difference between steady-state and oscillatory derivatives are appreciable for the 45° sweptback wing well below the force break, which is in contrast to results obtained for other derivatives (see ref. 4, for example) wherein differences in steady-state and oscillatory values were appreciable only at angles of attack near and above the force break.

Derivatives Due to Yawing Acceleration

The derivatives associated with yawing acceleration $C_{n_{\dot{r}}}$ and $C_{l_{\dot{r}}}$ are plotted against angle of attack in figure 7 for the three wings used in the investigation. For all three wings $C_{n_{\dot{r}}}$ was nearly zero at low angles of attack, and then increased at moderate and high angles of attack. At low α the parameter $C_{l_{\dot{r}}}$ increased negatively approximately linearly with angle of attack for all three wings. At angles of attack near and above maximum lift however, $C_{l_{\dot{r}}}$ for the unswept and 45° sweptback wing showed a rapid positive increase.

CONCLUSIONS

Preliminary tests have been made to determine effects of motion periodicity on the aerodynamic derivatives due to yawing velocity and acceleration for a 60° delta wing, a 45° sweptback wing, and an unswept

wing. The oscillation tests were made at one value of the reduced-frequence parameter, $\omega b/2V = 0.23$. Tests of models on other oscillating systems have shown a large dependence of some derivatives on the reduced frequency, particularly at high angles of attack, hence this fact should be kept in mind in considering the following statements:

1. At low angles of attack there was good agreement between steady-state and oscillatory values of the aerodynamic derivatives due to yawing velocity for all three wings.

2. At high angles of attack large differences occurred between steady-state and oscillatory values of the derivatives due to yawing velocity.

3. The derivatives due to yawing acceleration varied approximately linearly with angle of attack in the low-angle-of-attack range. At angles of attack near and above maximum lift, these derivatives showed no linear dependence on angle of attack, and attained large numerical values.

Langley Aeronautical Laboratory,
National Advisory Committee for Aeronautics,
Langley Field, Va., December 5, 1955.

[redacted]

APPENDIX

INSTRUMENTATION

Two quantities were measured by the instrumentation used in this investigation: the rolling moments and yawing moments acting on the model during forced oscillations in pure yawing. The moments were measured by means of resistance-type strain gages mounted on a strut support and attached to the model as indicated in figure 2. The moment outputs were modified by a sine-cosine resolver driven by the oscillating mechanism so that the output signals of the strain gage were proportional to the components of the strain-gage signals which were in-phase and out-of-phase with the model motion. The oscillation frequency was measured by use of a calibrated voltmeter driven by a generator attached to the oscillation equipment drive motor.

The components of the instrumentation were similar to those used in the investigation of reference 10. The arrangement of components, and the operation of the system were somewhat different however. The following sections explain the function and operation of the instrumentation used in the present investigation.

Theory of Instrumentation

A block diagram of the components of the instrumentation is shown in sketch (a).

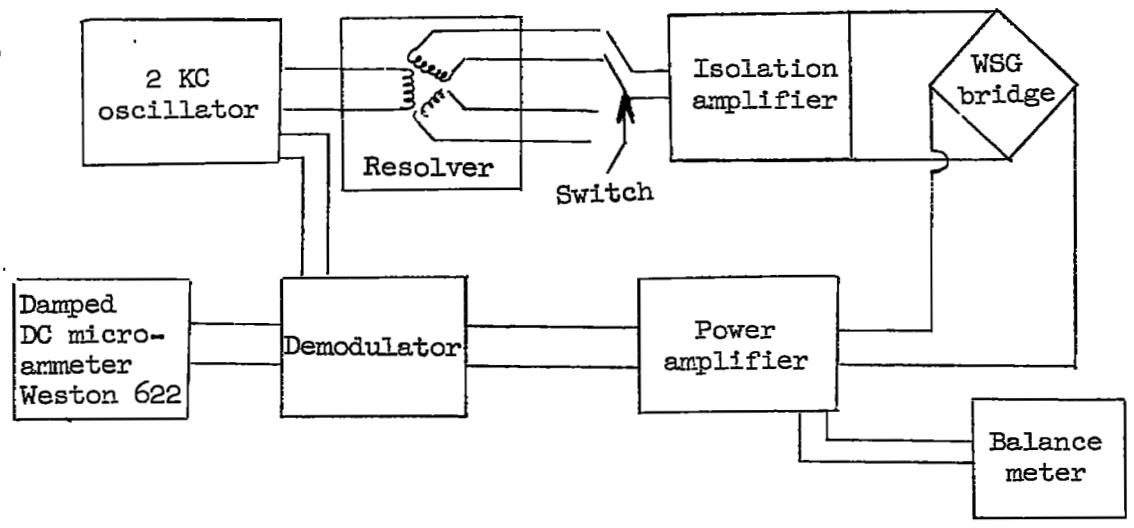

Sketch (a)

[redacted]

The output of one strain-gage element, for example, the yawing moment element, can be expressed as

$$e_n = K_n E n \tag{A1}$$

where

e_n output of strain-gage bridge, volts

K_n calibration factor of the balance, volts output per volt ft-lb

E strain-gage supply voltage, volts

n yawing moment applied to balance, ft-lb

The voltage E is obtained from a resolver attached to the shaft which drives the model-oscillating mechanism, and varies as the sine or the cosine of the shaft rotation angle $2\pi ft$. For the purpose of this discussion let

$$E = E_o \cos 2\pi ft \tag{A2}$$

where E_o is the maximum voltage at the strain-gage bridge from the resolver. Equation (A1) therefore can be written as

$$e_n = K_n E_o n \cos 2\pi ft$$

or

$$e_n = F_n n \cos 2\pi ft \tag{A3}$$

where $F_n = K_n E_o$, and is a calibration factor which relates the static strain-gage output e_n to the applied yawing moment n.

The aerodynamic yawing moment on the balance is given by

$$n = N_{\dot{\psi}} \dot{\psi} + N_{\ddot{\psi}} \ddot{\psi} \tag{A4}$$

Substituting equation (A4) into (A3) and using equations (8) and (9) of the text to eliminate $\dot{\psi}$ and $\ddot{\psi}$ yields

[redacted]

$$e_n = F_n \cos 2\pi ft \left[-N_{\dot{\psi}}^{\cdot} \frac{4\pi fR}{l} \cos 2\pi ft + N_{\dot{\psi}} \frac{8\pi^2 f^2 R}{l} \sin 2\pi ft \right] \tag{A5}$$

If the strain-gage output e_n is applied to a low-frequency, well-damped direct-current meter which will not respond appreciably to frequencies near the test oscillation frequency f, the average voltage $\bar{e}_n$ indicated by the meter is

$$\bar{e}_n = \frac{1}{t} \int_0^t e_n dt \tag{A6}$$

Substitution of equation (A5) into equation (A6) and integrating yields

$$\bar{e}_n = F_n \frac{2\pi fR}{l} N_{\dot{\psi}}^{\cdot} \tag{A7}$$

from which

$$N_{\dot{\psi}}^{\cdot} = \frac{l\bar{e}_n}{2\pi fRF_n} \tag{A8}$$

A comparison of equations (A5) and (A7) shows that $\bar{e}_n$ is exactly one-half of the value of e_n when the resolver is in such a position so as to eliminate the derivative not being measured. In other words, the oscillatory value of e_n is one-half the maximum value of the static e_n for either the in-phase or out-of-phase component. This relationship is useful since it permits a static rather than dynamic calibration of the instrumentation.

The derivative $N_{\dot{\psi}}$ is obtained in a manner similar to that used in obtaining $N_{\dot{\psi}}^{\cdot}$, by using the sine rather than cosine component of the resolver. In this case the equation obtained is

$$N_{\dot{\psi}} = \frac{l\bar{e}_n}{4\pi^2 f^2 RF_n} \tag{A9}$$

[redacted]

Equations (A8) and (A9) can be nondimensionalized to obtain the desired derivatives

$$C_{n_r} = \frac{2\bar{e}_n}{\pi^2 f^2 R\rho b^2 S F_n} \tag{A10}$$

and

$$C_{n_{\dot{r}}} = \frac{2\bar{e}_n l}{\pi^2 f^2 R\rho S b^3 F_n} \tag{A11}$$

The value of $\bar{e}_n$ used in the equations is, of course, the value due to aerodynamic forces. Effects of inertia are eliminated by subtracting wind-off values from wind-on values.

Equipment

A block diagram of the electronic equipment used is shown as sketch (a). The resolver is a Reeves type R600 resolver and is powered by a 2000-cps oscillator. This frequency was selected because it resulted in a minimum phase shift between the input and output of the resolver and hence also resulted in a maximum output of the phase-sensitive demodulator.

The sine or the cosine output of the resolver can be switched into the two-stage isolation amplifier. The amplifier, which has a gain of two, prevents loading of the resolver by the wire strain gage thus insuring minimum distortion in the voltage powering the strain gage.

The output of the wire strain gage is put into a two-stage amplifier in order to obtain sufficient input into the phase-sensitive half-wave demodulator with the low loads obtained on the balance in the present investigation. The demodulator output is read on a damped direct-current microammeter.

Possible Errors Associated with Reduction of Data

Referring to equations (A5) and (A7), it is seen that the electrical multiplying and integrating processes eliminate the signals not in phase with the reference voltage, E. Consider the following unwanted moments which the balance senses:

[redacted]

(a) Aerodynamic moments due to harmonics of basic model motion due to linkage.- Harmonics such as $\cos 2\omega t$, $\cos 3\omega t$, etc., being of different frequency from the reference voltage, are eliminated.

(b) Aerodynamic moment due to misalinement of model with airstream.- This causes a constant moment on the balance. Since the voltage to the balance is reversed each half cycle, the balance output is also reversed and averages zero.

(c) Turbulence in airstream.- All components not of the same frequency as the reference voltage are eliminated. Theoretically, if the turbulence is truly random, components at or close to the reference frequency are also eliminated. Practically, if these components are of appreciable magnitude, the indicator will fluctuate slowly, and it is necessary that these fluctuations be averaged out by eye over a long period of time.

(d) Vibration of model on balance.- The natural frequency of the model-balance combination should be as much above the reference frequency as possible. The comments of (c), above, apply.

(e) Angular acceleration of the model.- This is exactly in phase with the acceleration derivatives. The moments due to inertia of the model are determined by oscillating the model while it is enclosed in a box, and are then subtracted from the test reading to give the aerodynamic moments.

(f) Linear acceleration of the model.- The linear acceleration is given approximately by $\ddot{y} = -4\pi^2 f^2 R \cos 2\pi f t$, which is in phase with $\dot{\psi}$ and hence affects the yawing velocity derivatives if the model is not mass balanced about the moment center. The increments in moments due to this source are eliminated by wind-off tests as explained in (e). Other sources of error lie in the equipment used:

(g) Harmonics in strain-gage supply voltage.- These will pick up any moments on the balance of corresponding frequencies and cause errors in the data proportional to the magnitude of the harmonics present. It is, therefore, important that the strain-gage supply voltage be as pure a sine or cosine wave as possible in order to be consistent with the accuracy desired in the test data.

(h) Balance zero drift.- This is usually very slow compared to the model oscillation and the comments of (b), above, apply.

[redacted]

(i) Phase error in strain-gage supply voltage.- As an example, the sine and cosine output windings of the resolver used in these tests are 90° apart within ± 3 minutes. It was possible to statically set the zero in the sine output winding of the resolver within ± 10 minutes of zero model position. With a 20:1 ratio of in-phase to out-of-phase component of the moment, and a 13-minute error in alinement, the out-of-phase reading will have an 8-percent error due to misalinement.

(j) Unbalanced demodulator.- This is a definite source of error as it can cause a reading on the indicator with no output from the strain gages. During these tests the demodulator was balanced carefully after a warmup period and was then checked (and readjusted, if necessary) periodically during each run with the strain gages disconnected.

REFERENCES

1. Fisher, Lewis R., and Fletcher, Herman S.: The Effect of Lag of Sidewash on the Vertical-Tail Contribution to Oscillatory Damping in Yaw of Airplane Models. NACA TN 3356, 1955.

2. Hewes, Donald E.: Low-Speed Measurement of Static Stability and Damping Derivatives of a 60° Delta-Wing Model for Angle of Attack of 0° to 90°. NACA RM L54G22a, 1954.

3. Johnson, Joseph L., Jr.: Low-Speed Measurements of Rolling and Yawing Stability Derivatives of a 60° Delta-Wing Model. NACA RM L54G27, 1954.

4. Riley, Donald R., Bird, John D., and Fisher, Lewis R.: Experimental Determination of the Aerodynamic Derivatives Arising From Acceleration in Sideslip for a Triangular, a Swept, and an Unswept Wing. NACA RM L55A07, 1955.

5. Bird, John D., Jaquet, Byron M., and Cowan, John W.: Effect of Fuselage and Tail Surfaces on Low-Speed Yawing Characteristics of a Swept-Wing Model As Determined in Curved-Flow Test Section of the Langley Stability Tunnel. NACA TN 2483, 1951. (Supersedes NACA RM L8G13.)

6. Silverstein, Abe, and White, James A.: Wind-Tunnel Interference With Particular Reference to Off-Center Positions of the Wing and to the Downwash at the Tail. NACA Rep. 547, 1936.

7. Evans, J. M.: Stability Derivatives. Wind Tunnel Interference on the Lateral Derivatives l_p, l_r, and l_v With Particular Reference to l_p. Rep. ACA-33, Australian Council for Aeronautics, Mar. 1947.

8. Runyan, Harry L., Woolston, Donald S., and Rainey, A. Gerald: Theoretical and Experimental Investigation of the Effect of Tunnel Walls on the Forces on an Oscillating Airfoil in Two-Dimensional Subsonic Compressible Flow. NACA TN 3416, 1955. (Supersedes NACA RM L52I17a).

9. Campbell, John P., Johnson, Joseph L., Jr., and Hewes, Donald E.: Low-Speed Study of the Effect of Frequency on the Stability Derivatives of Wings Oscillating in Yaw With Particular Reference to High Angle-of-Attack Conditions. NACA RM L55H05, 1955.

[redacted]

10. Lessing, Henry C., Fryer, Thomas B., and Mead, Merrill H.: A System for Measuring the Dynamic Lateral Stability Derivatives in High-Speed Wind Tunnels. NACA TN 3348, 1954.

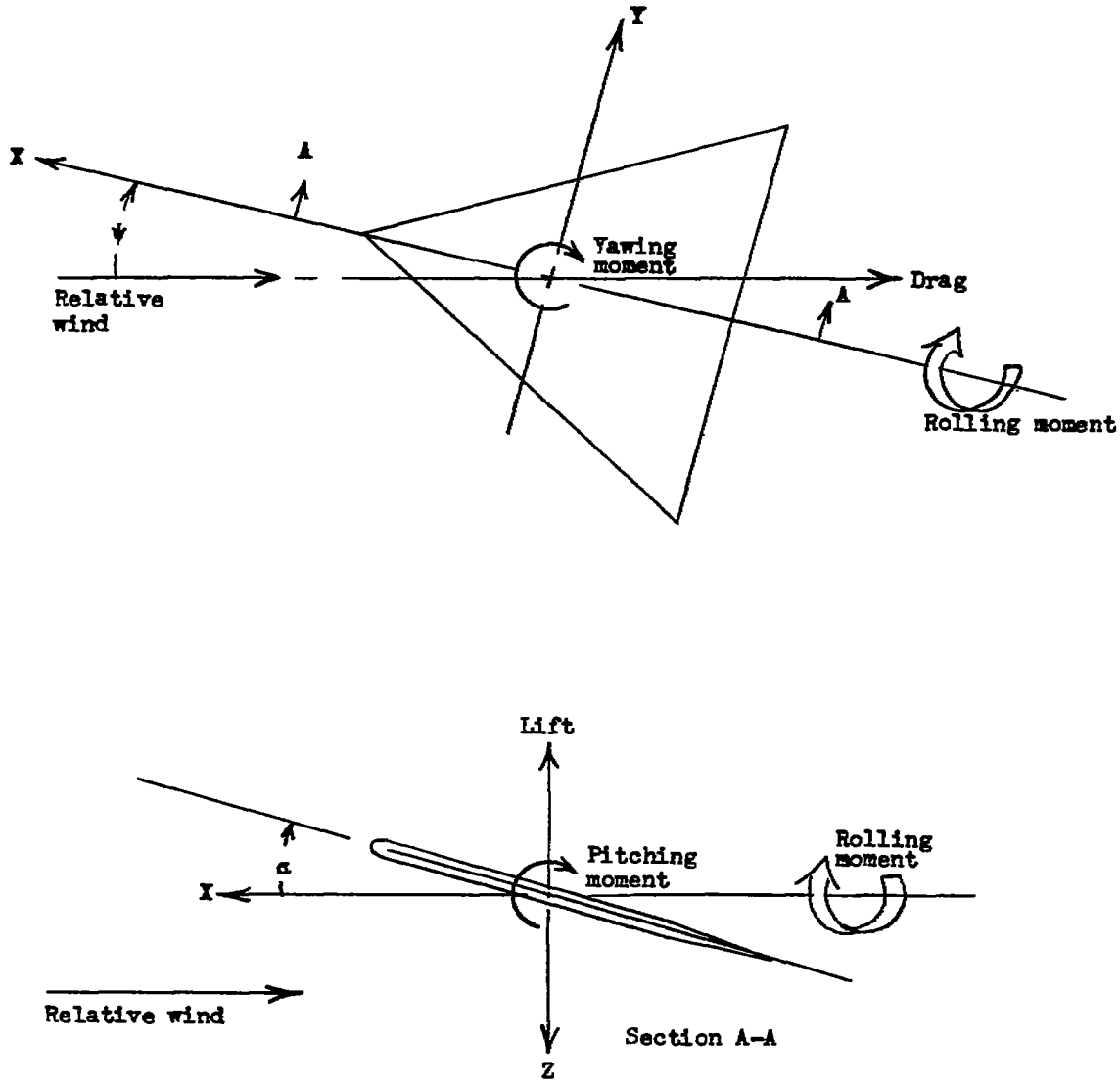

Figure 1.- System of stability axes. Arrows indicate positive forces, moments, and displacements.

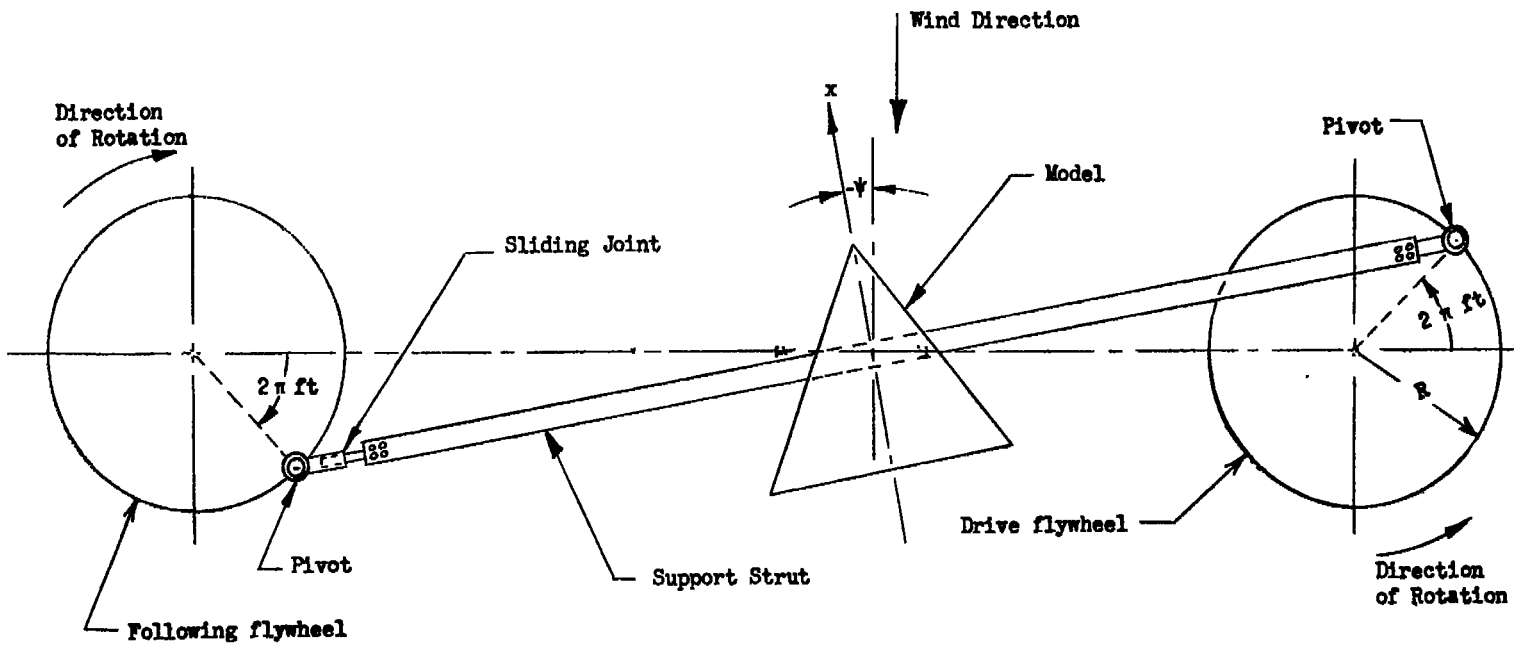

(a) Top view.

Figure 2.- Schematic drawing of mechanism for simulating pure yawing oscillation.

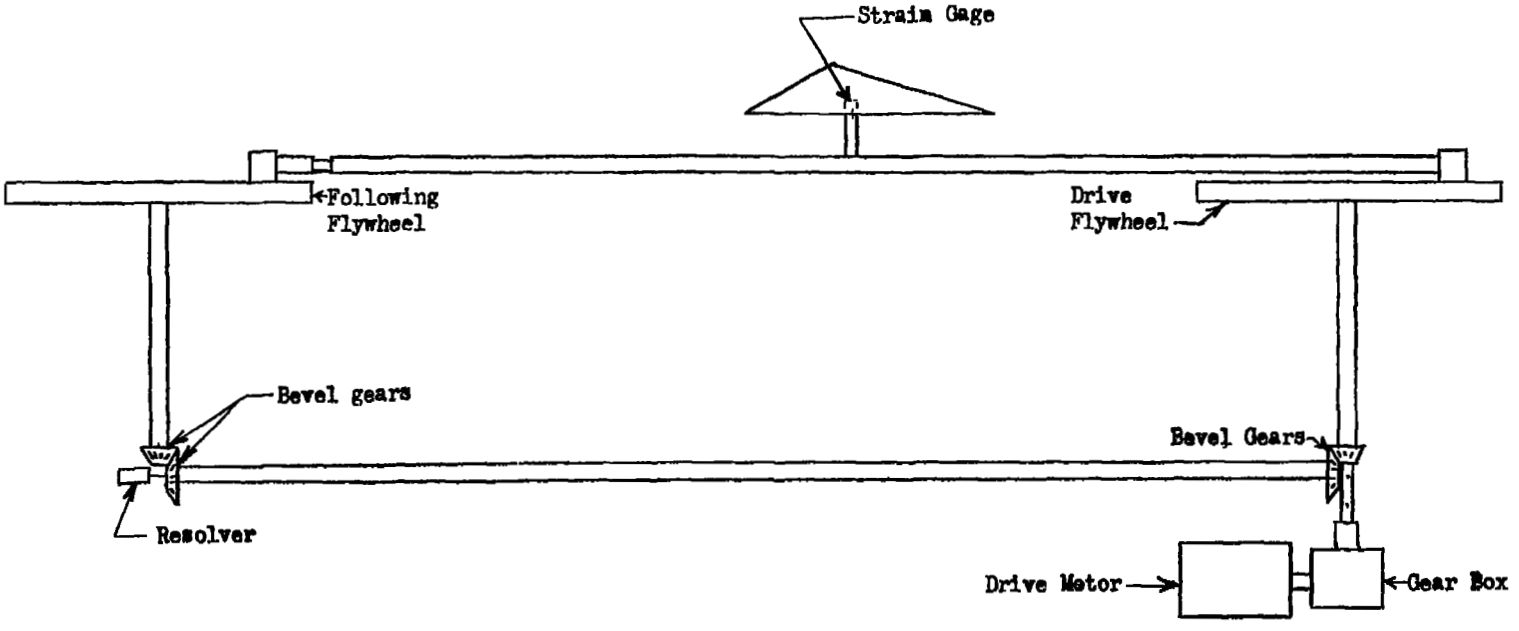

(b) View looking upstream.

Figure 2.- Concluded.

L-87045

(a) Driving flywheel.

Figure 3.- Apparatus used in obtaining pure yawing oscillation.

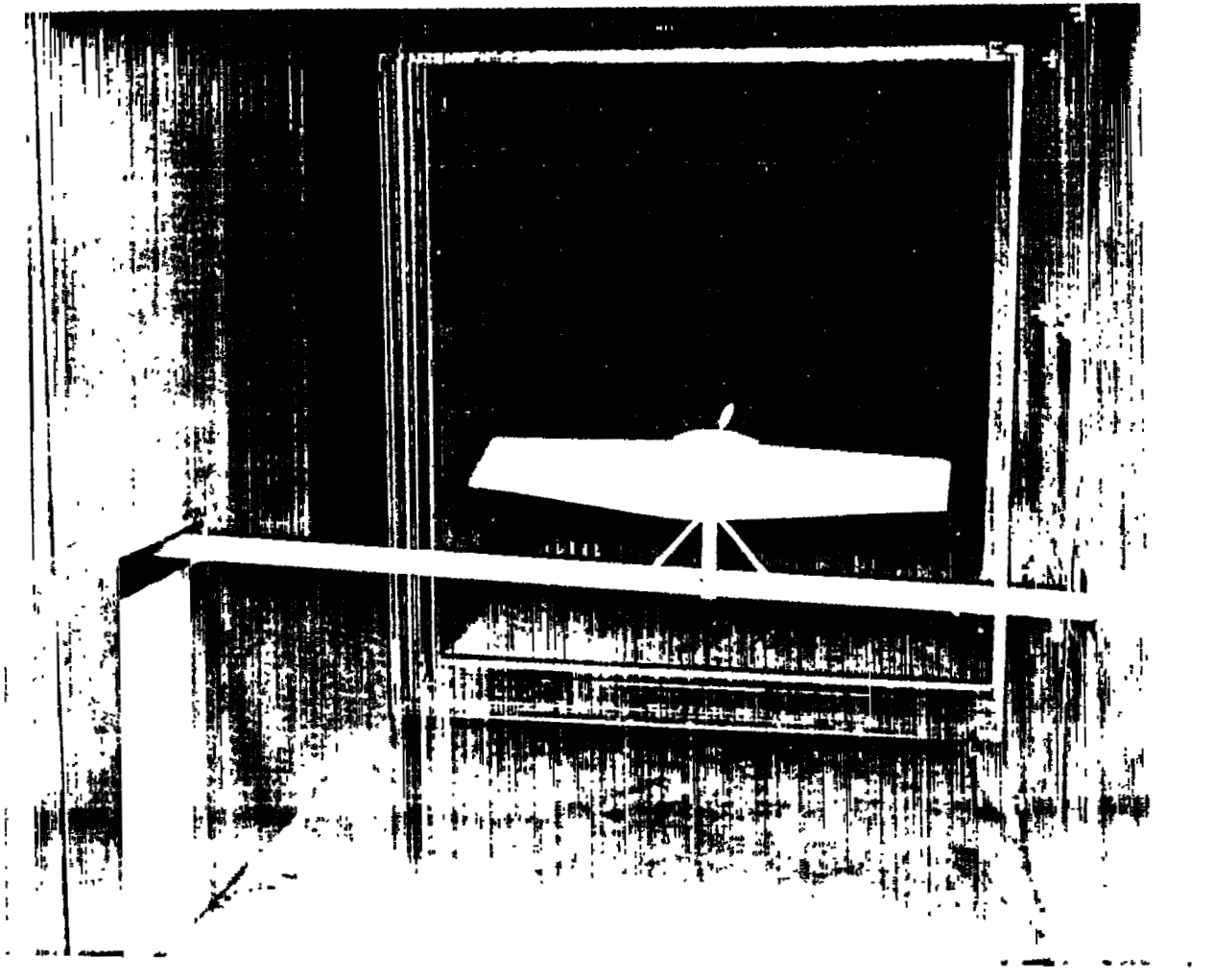

L-87046

(b) Model support strut and unswept wing.

Figure 3.- Continued.

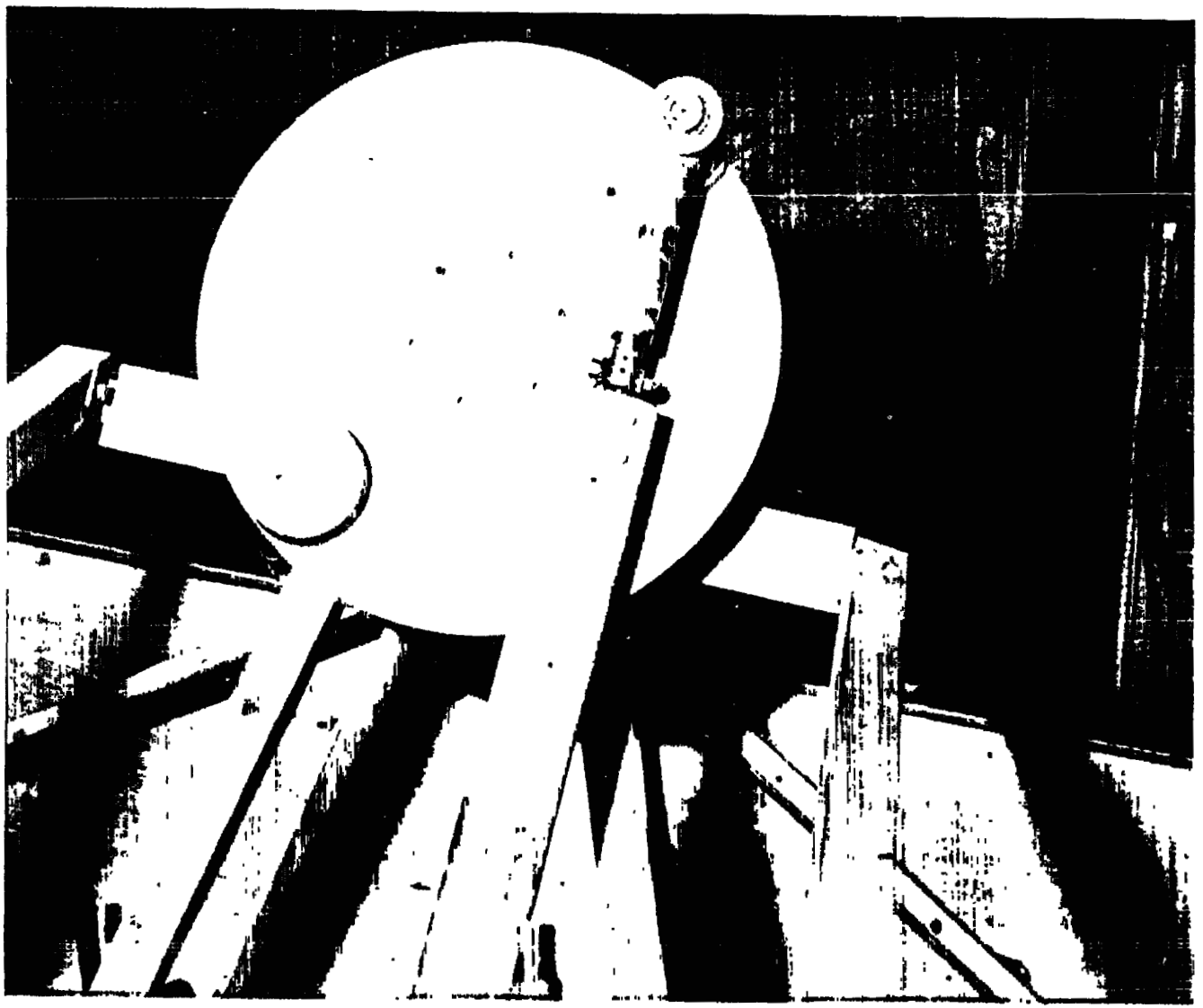

L-87162

(c) Top view of following flywheel.

Figure 3.- Continued.

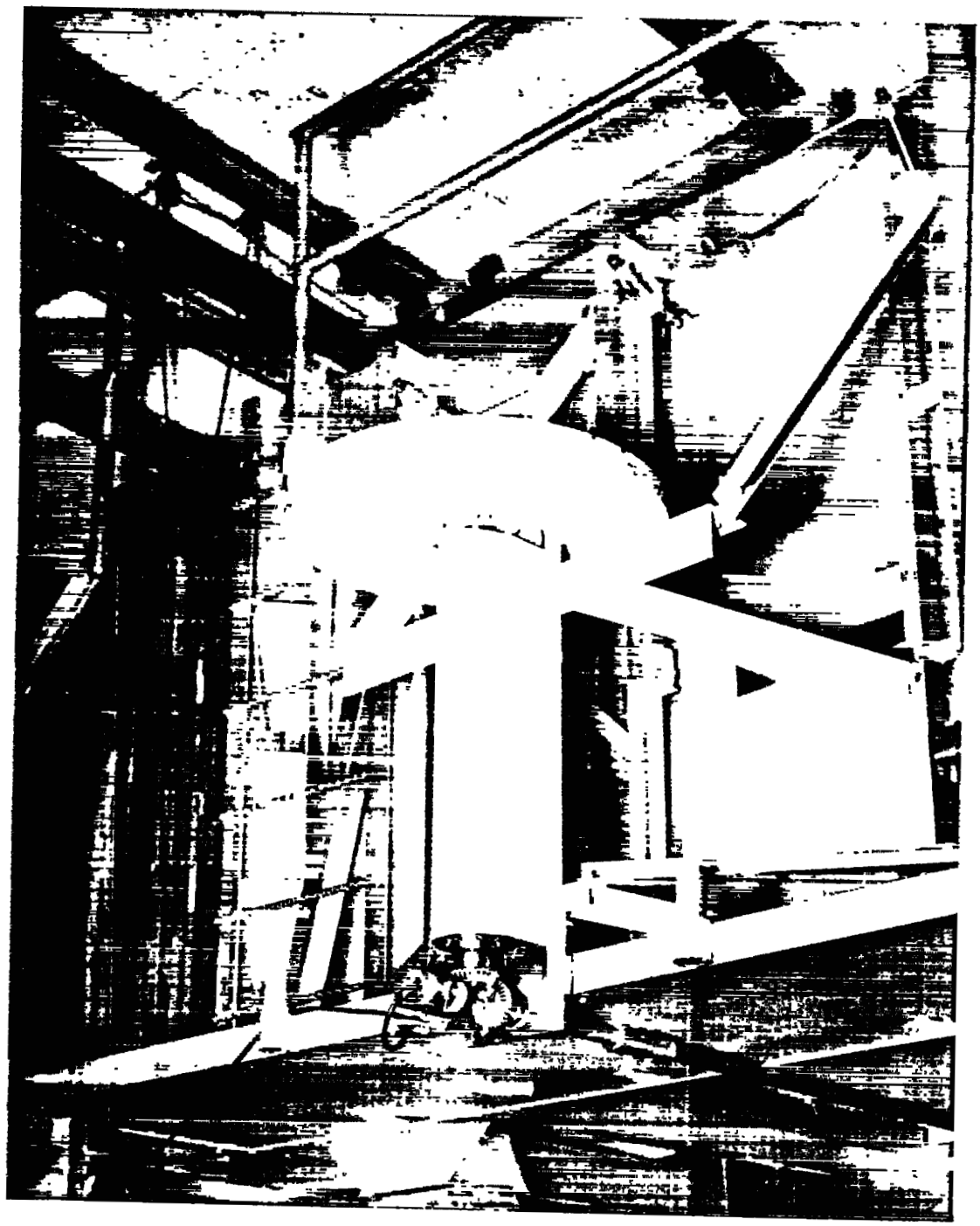

(d) Side view of following flywheel. L-87163

Figure 3.- Concluded.

[redacted]

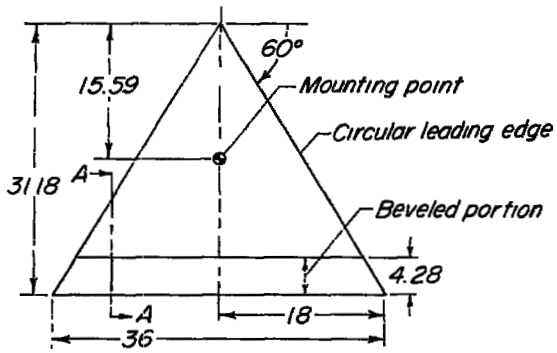

Delta wing

Aspect ratio	2.31
Leading-edge sweep angle, deg.	60
Dihedral angle, deg.	0
Twist, deg.	0
Airfoil section	Flat plate
Area, sq. in.	561.20
Span, in.	36.00
Mean aerodynamic chord, in.	20.79

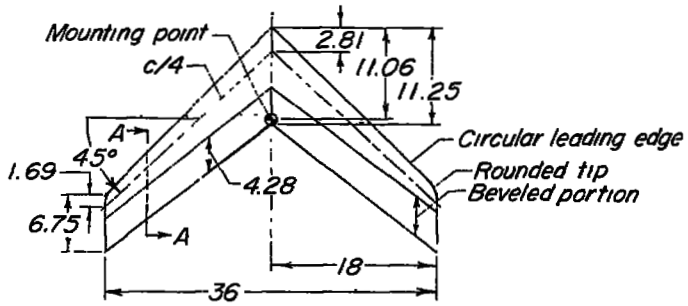

Swept wing

Aspect ratio	4.0
Taper ratio	0.6
Quarter chord sweep angle, deg.	45
Dihedral angle, deg.	0
Twist, deg.	0
Airfoil section	Flat plate
Area, sq. in.	324
Span, in.	36
Mean aerodynamic chord, in.	9.19

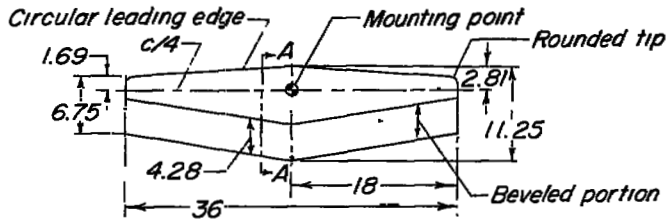

Unswept wing

Aspect ratio	4.0
Taper ratio	0.6
Quarter chord sweep angle, deg.	0
Dihedral angle, deg.	0
Twist, deg.	0
Airfoil section	Flat plate
Area, sq. in.	324
Span, in.	36
Mean aerodynamic chord, in.	9.19

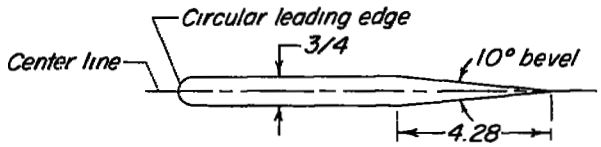

Section A-A

Figure 4.- Sketches and geometric characteristics of the three wing models investigated. All dimensions are in inches.

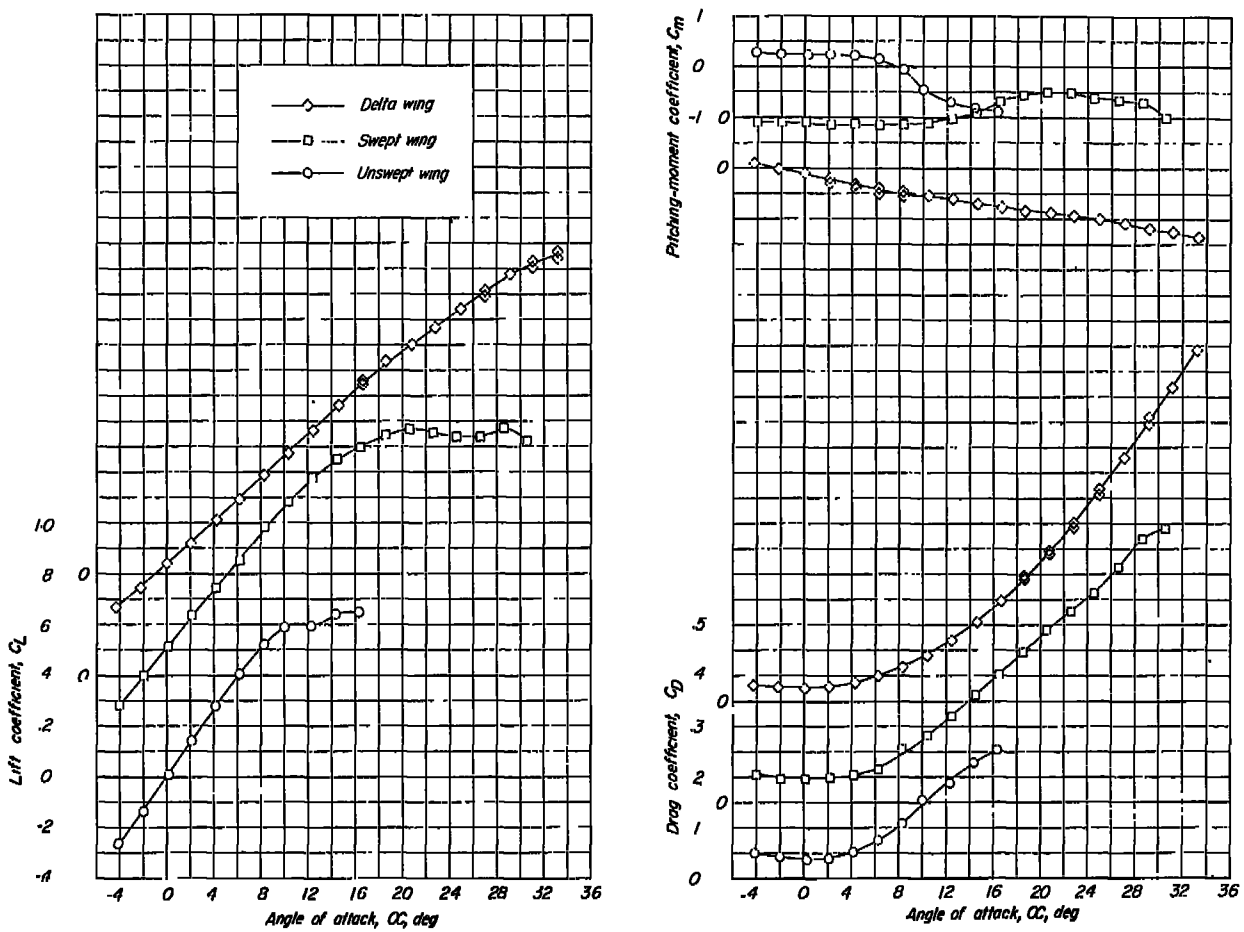

Figure 5.- Lift, drag, and pitching-moment characteristics of wings used in investigation.

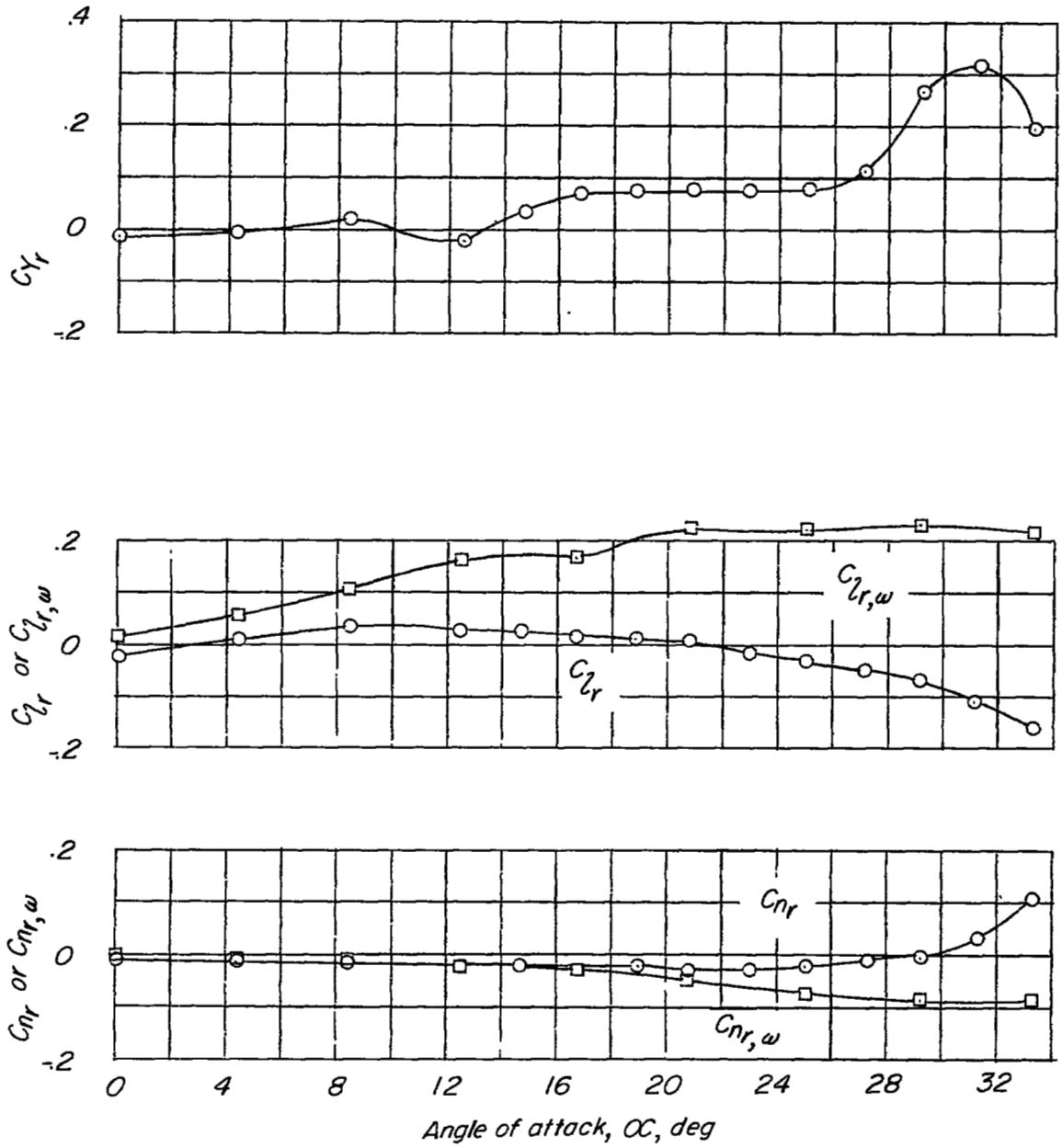

(a) 60° delta wing.

Figure 6.- Comparison of values of the derivatives due to yawing velocity from steady-state and oscillation tests.

[redacted]

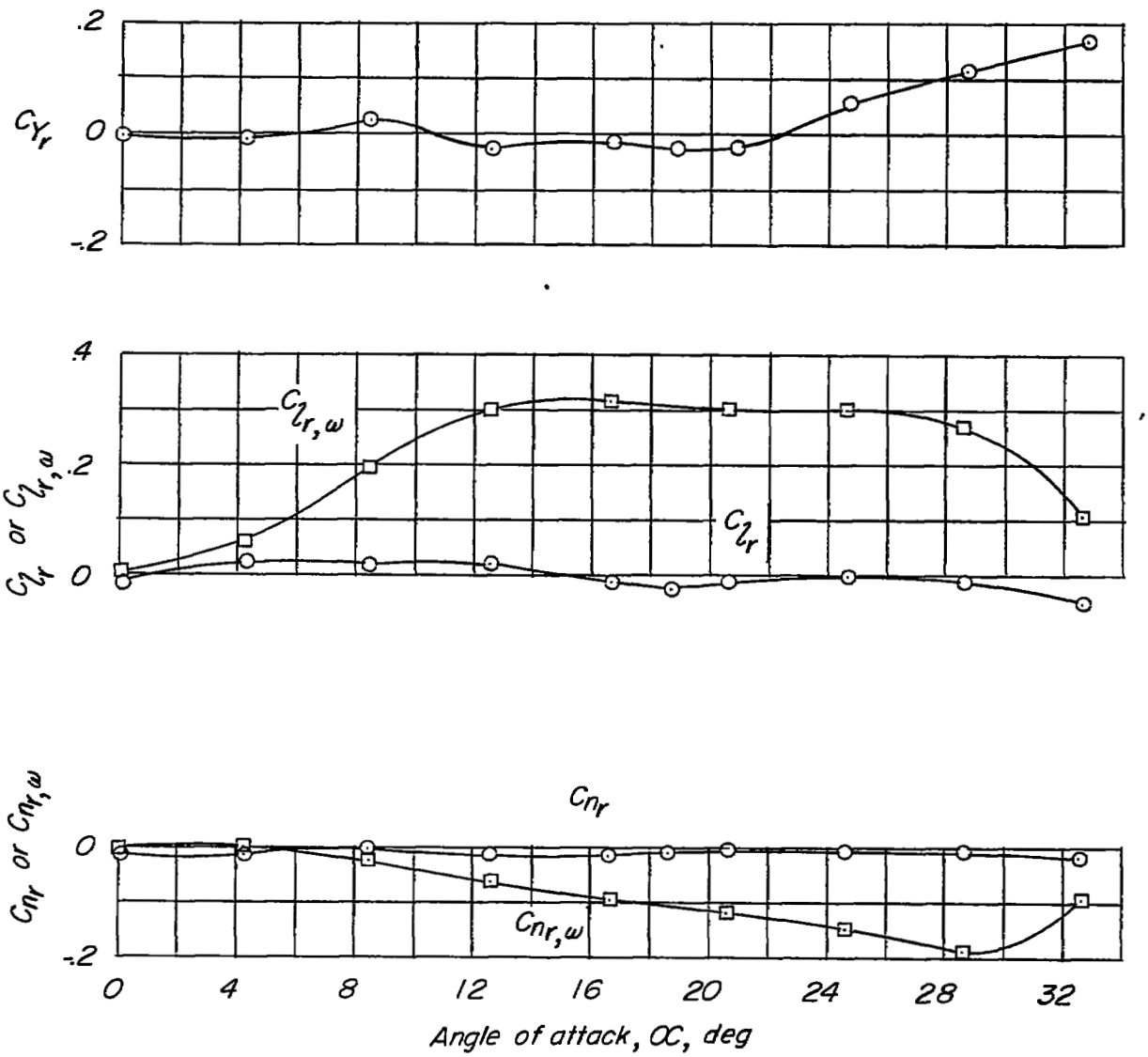

(b) 45° sweptback wing.

Figure 6.- Continued.

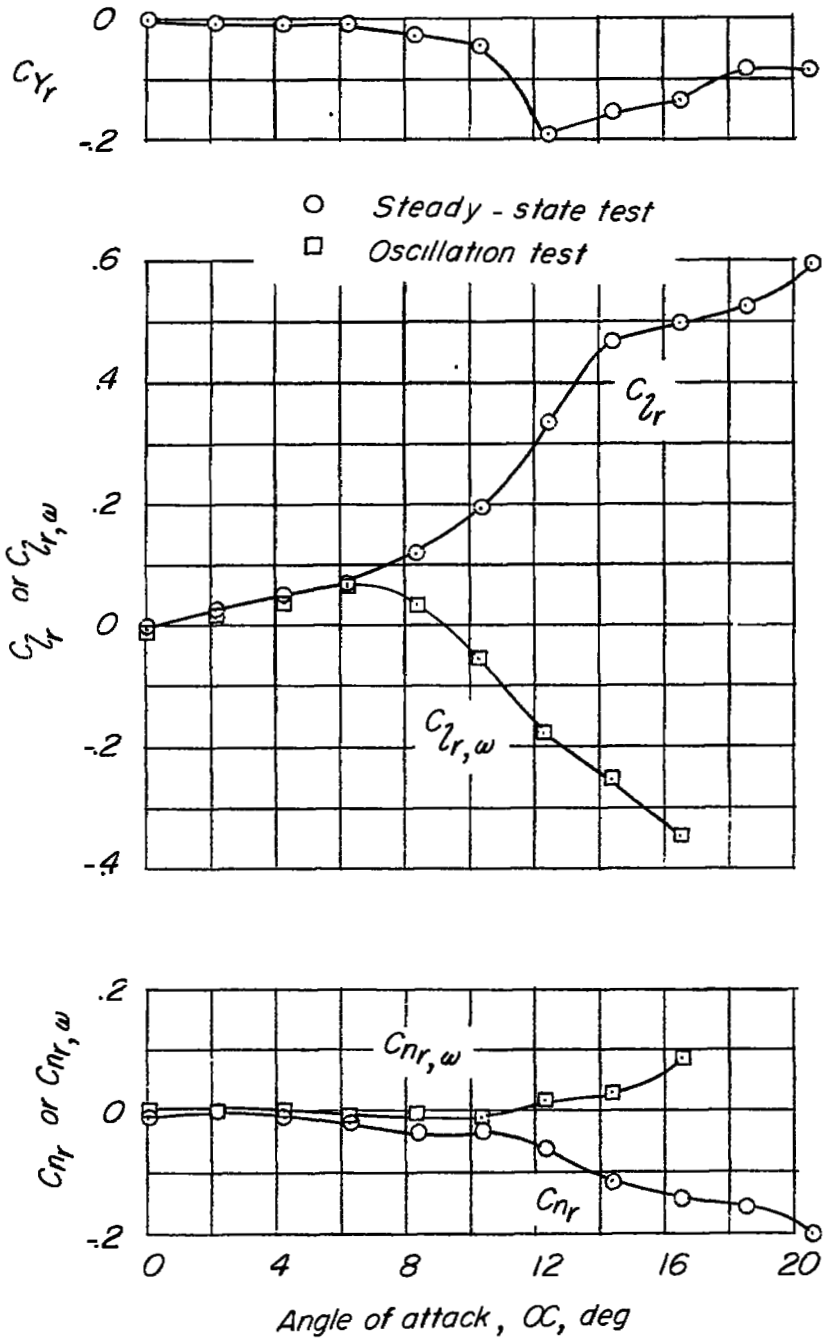

(c) Unswept wing.

Figure 6.- Concluded.

[redacted]

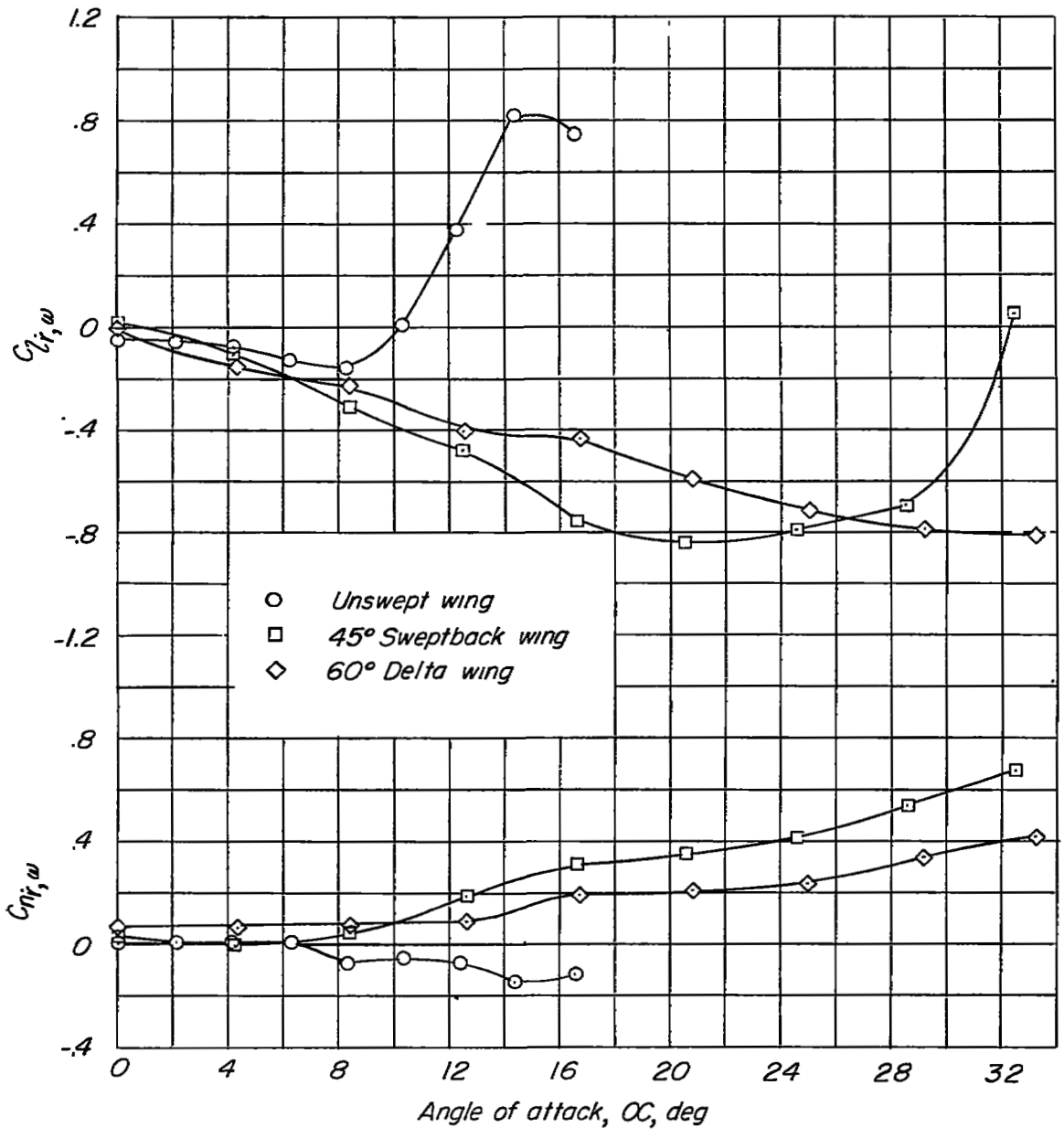

Figure 7.- Derivatives due to yawing acceleration for the three wings tested.

NACA - Langley Field, Va.